

**A simulation-based model studying monoethanolamine and Aprotic Heterocyclic Anion
Ionic Liquid (AHA-IL) mixtures for carbon capture**

Adhish Chandra Saketh Madugula¹, Clayton Jeffryes¹, James Henry¹, John Gossage¹, and Tracy
J. Benson^{1‡}

¹Dan F. Smith Department of Chemical and Biomolecular Engineering, Lamar University, P.O.
Box 10053, Beaumont, TX, USA

[‡]Person to whom correspondence should be addressed

Phone: +1 (409) 880 – 7536

Email: tracy.benson@lamar.edu

Abstract

Capturing of waste CO₂, particularly from large industrial point sources, is necessary for either permanent storage or CO₂ utilization. Amine solvents used for carbon capture have certain drawbacks, particularly the high energy required by the reboiler for solvent regeneration and degradation of the amine with absorption/regeneration cycling. These challenges may be overcome using ionic liquids (ILs) that can be tailored for operating under typical flue gas stream conditions (8–10% CO₂, 18–20% H₂O, 2–3% O₂, and 67–72% N₂). ILs, however, oftentimes suffer from high viscosities, leading to diffusion limitations when compared to amine solvents. This work models the combinations of aprotic heterocyclic anion ILs (AHA-IL) with monoethanolamine (MEA) and studies the carbon capture effectiveness of these mixtures. This study found that all AHA-IL/MEA mixtures exhibited 32 % lower enthalpy of reaction (compared to MEA) and 64 % lower viscosity (compared to AHA-IL), which are desirable characteristics for CO₂ capture solvents.

Keywords: Carbon Capture, Ionic Liquid, Monoethanolamine, Viscosity, Absorption Capacity

1. Introduction

The primary source of energy since the onset of the industrial revolution has been fossil-based feedstocks. These feedstocks (i.e., coal, crude petroleum, and natural gas) have been the primary driver for growing economies, increasing standards of living, and advancing technologies. However, the use of these feedstocks has caused significant increases in atmospheric CO₂ levels (American Chemical Society, 2013). According to the U.S. EPA, 76 % of all CO₂ emissions from industrial sources in the U.S. in 2018 was from fossil fuel combustion. Among these sources, electric power plants, oil and gas processes, chemical production facilities, and petroleum refineries were identified as the primary large point sources of CO₂ emissions (US-EPA, 2022; Madugula et al., 2021). Therefore, developing solutions to reduce CO₂ emissions from industrial sources has become paramount in providing a long term, sustainable global ecosystem.

Currently, the most mature and utilized technology for post-combustion CO₂ capture, compression, and dehydration uses an aqueous solution of 30 wt % monoethanolamine (MEA) for CO₂ capture (Luis, 2016; Nittaya et al., 2014). However, amine-based solvents have high operational expenses, as they are plagued with thermal degradation, degeneration in the presence of impurities (O₂, SO_x, and NO_x), high regeneration energy requirements, and loss of solvent during regeneration (Davis and Rochelle, 2009; Fredriksen and Jens, 2013; Zhou et al., 2012). Hence, alternative solvents such as Ionic Liquids (ILs) have caught the interest of the scientific community for their intrinsic properties, including negligible volatility, high CO₂ absorption, and low corrosivity (Davis and Rochelle, 2009; Fredriksen and Jens, 2013; Zhou et al., 2012). However, ILs also come with their own drawbacks, including high viscosity and ineffectiveness in the presence of water. The high viscosity of ILs is especially detrimental to the application of

ionic liquids as alternative CO₂ capture solvents as it fosters lower reaction kinetic rates, poor mass transfer rates, increases the energy requirement for pumping the liquid, and causes elevated energy requirements during CO₂ regeneration. Therefore, decreasing the viscosity of the ionic liquid would improve the diffusivity of the CO₂ molecule, thereby increasing the diffusion coefficient. The dependence of viscosity on the diffusion coefficient can be quantified using the Wilke – Chang equation (Eq 1) (AspenTech, 2019; Poling et al., 2001).

$$D_{ij} = 1.173 \times 10^{-16} \left(\frac{T \times \sqrt{\phi_j \times MW_j}}{\mu_j \times (V_{bi})^{0.6}} \right) \quad \text{Eq 1}$$

where, **i** refers to the diffusing solute, **j** refers to the solvent.

D_{ij} = Diffusion Coefficient of solute, i, into solvent, j, (m²/s)

T = Temperature of the solution (K)

φ_j = Association Factor for solvent (= 1)

MW_j = Molecular weight of solvent

V_{bi} = Liquid molar volume at boiling point of solute, i, (m³/kmol)

μ_j = Liquid viscosity of solvent, j, (kg/(m.s))

Unfortunately, many ILs have also shown increased viscosity upon saturation with CO₂, severely limiting mass transfer during CO₂ capture (Anderson et al., 2007; Brennecke and Gurkan, 2010; Garip and Gizli, 2020; Lei et al., 2017; Lian et al., 2021; Park et al., 2015; Ramdin et al., 2012; Torralba-Calleja et al., 2013), resulting in negative diffusion impacts. A new class of ILs containing aprotic heterocyclic anions (AHAs) were recently discovered that do not exhibit increased viscosity with CO₂ saturation. This phenomenon is due to the absence of the H⁺ ion in the anion, preventing the IL from forming intramolecular hydrogen bonds (Gurkan

et al., 2010; Seo et al., 2014). Additionally, when these AHAs were paired with a phosphonium cation, the IL maintained CO₂ absorption performance even in the presence of water (Gurkan et al., 2010; Seo et al., 2014). Thereby making phosphonium based AHA-ILs suitable for post combustion flue gas conditions in which a high-water content (> 10% by wt.) is typically expected.

In particular, the AHA-ILs, triethyloctylphosphonium 2-cyanopyrrolide, [P2228][2-CNPyr], and trihexyltetradecylphosphonium 2-cyanopyrrolide, [P66614][2-CNPyr], (**Figure 1**) have shown promising results as potential replacements for amine – based solvents. Both ILs have shown to reach an absorption capacity of ~ 1 mol CO₂/mol of IL [24]. However, their viscosities are 80 and 160 cP, respectively, compared to ~ 7 cP for amine solvents at typical post combustion capture conditions (Maham et al., 2002). One way to reduce viscosity of the AHA-ILs is using a co-solvent. This was demonstrated by de Riva et al (2018), where [P66614][2-CNPyr] and [P66614][2-CNPyr] were diluted up to 25 wt % using tetraglyme. The tetraglyme-IL hybrid solvent preserved the CO₂ absorption capacity of the IL while decreasing the viscosity of the solvent (de Riva et al., 2018; Hospital-Benito et al., 2021, 2020). However, as tetraglyme has low absorption CO₂ capacity, the authors of this paper believe that utilization of a co-solvent with better CO₂ absorption could result in a hybrid solvent system with improved CO₂ absorption capacity and lower viscosity.

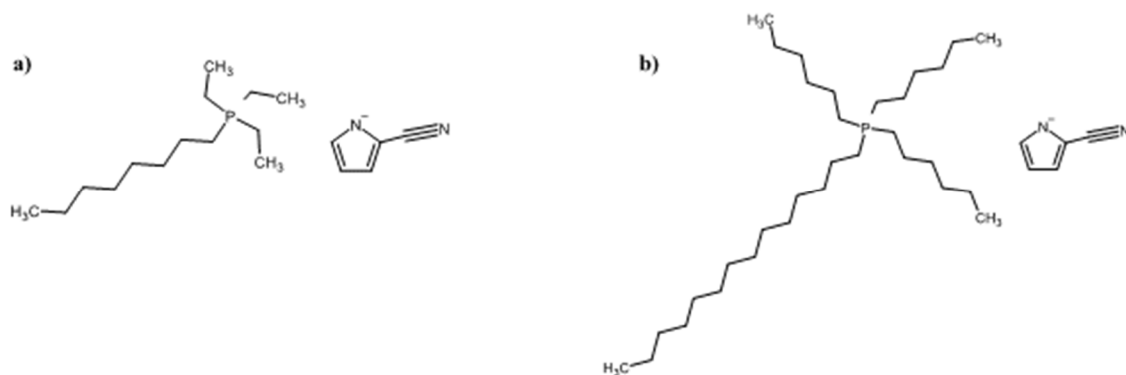


Figure 1: (a) Molecular Structure of triethyloctylphosphonium 2-cyanopyrrolide, [P2228][2-CNPyrr] and (b) trihexyltetradecylphosphonium 2-cyanopyrrolide, [P66614][2-CNPyrr]

Hence, the authors of this study suggest the use of MEA as a co-solvent with AHA-IL. The ionic liquids, [P2228][2-CNPyrr] and [P66614][2-CNPyrr], were chosen in this study to represent the phosphonium based AHA-ILs. The authors of this work hypothesize that using MEA to dilute AHA-ILs would improve the CO₂ absorption by two methods 1) decreasing the viscosity to improve CO₂ diffusivity and 2) increasing CO₂ reactivity and reducing the dilution effect by providing two chemical routes for CO₂ capture in the solvent instead of just one. The first chemical route would be through the formation of ILCOO complex formed by the reaction of the 2-cyano-carbonitrile anion of the ionic liquid and CO₂ (**Figure 2**), and the second route would be through the formation of a carbamate ion due to MEA. Additionally, based on the work of de Riva et al. (2020), the addition of 30 wt % aqueous amine was also studied as the authors hypothesize that the water in the MEA solution would help absorb the heat generated due to the exothermic nature AHA-IL/MEA/CO₂ interactions.

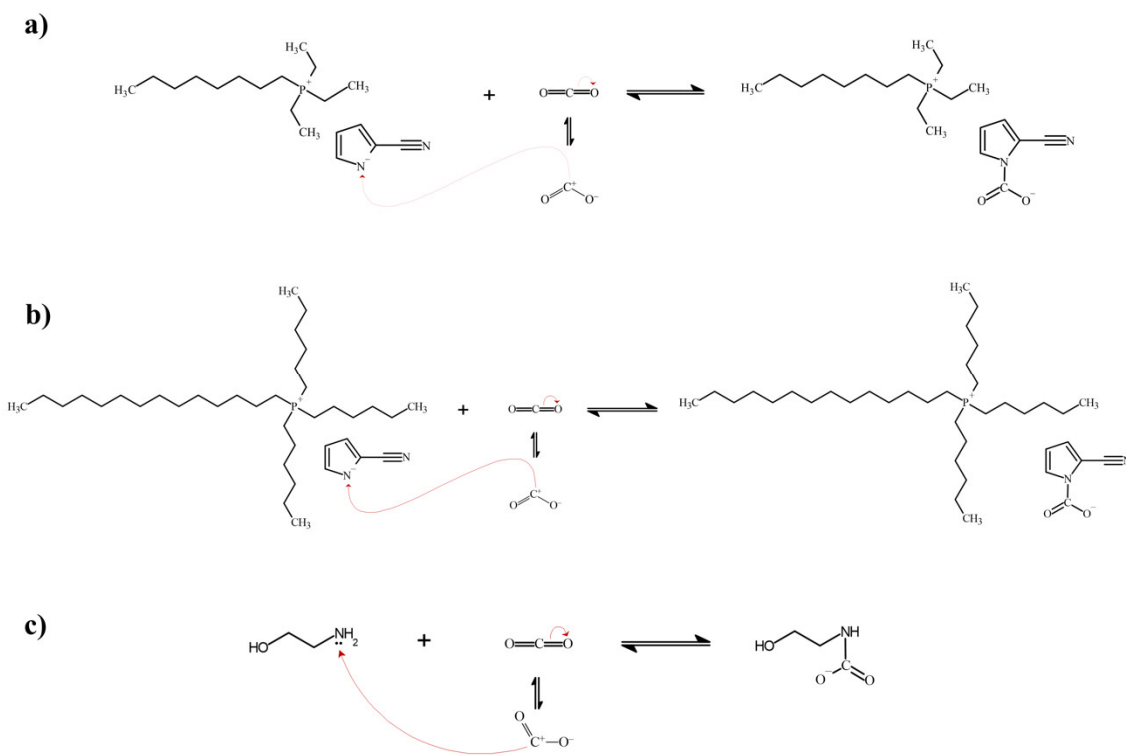


Figure 2: Reaction Mechanism for CO₂ with (a) [P2228][2-CNPyrr], (b) [P66614][2-CNPyrr] and (c) ethanolamine (C₂H₄NH₂OH) and CO₂

There are only a handful of studies using MEA as a cosolvent to dilute ILs despite having favorable results. For example, the CO₂ absorption capacity of 1-butyl-3-methylimidazolium acetate and 1-ethyl-3-methylimidazolium octylsulfate mixed with aqueous MEA was linearly dependent on the concentration of MEA. The water in the mixture facilitated the decrease of viscosity of the solvent complex (Baj et al., 2013). Yang et al. (2014) studied the effect of aqueous MEA with 1-Butyl-3-methylimidazolium tetrafluoroborate, [bmim][BF₄], to reduce the energy consumption and operating costs of CO₂ capture from low-pressure flue gas streams. The regeneration energy was reduced by ~ 37 % for MEA/[bmim][BF₄]/H₂O (0.3:0.4:0.3 w/w/w) mixture and MEA loss was reduced by 50 % compared to that of traditional aqueous amine-

based CO₂ capture. The mixed IL also had a low viscosity (3.54 cP), facilitating the application of IL-based solvents in industrial applications [31]. Additionally, there are no studies found in the open literature studying the effect of MEA on AHA-ILs.

Hence, this study, provides a unique perspective by presenting a model study on the effect of aqueous and nonaqueous MEA on [P2228][2-CNPy_r] and [P66614][2-CNPy_r] using process modeling software and proposes a suitable MEA and IL composition for low viscosity and low reaction enthalpy. These parameters were chosen for optimum absorption/solvent regeneration efficiency. The energy required for solvent regenerate depends on the enthalpy of reaction between CO₂ and the solvent. Therefore, the desired hybrid solvent should possess low enthalpy of reaction, preferably be lower than that of MEA (-85 kJ/mol of CO₂ absorbed).

2. Simulation Methodology

The effect of the addition of nonaqueous MEA and aqueous MEA to [P2228][2-CNPy_r] and [P66614][2-CNPy_r] on viscosity and CO₂ absorption capacity was studied using Aspen Plus[®] v11 software package. Although a CO₂ capture study usually uses an absorber column for solvent-based CO₂ capture, in this work the authors used an adiabatic continuously stirred tank reactor (CSTR) to study the chemical reactions between IL, MEA, and CO₂. This provided a good approximation as each tray in an equilibrium-based reactive absorber is equivalent to a CSTR.

The Electrolytic Non-Random Two Liquid – Redlich Kwong (ENRTL–RK) thermodynamic package was used in this study to account for the IL/MEA/H₂O/CO₂ electrolyte system (Akinola et al., 2019; Sanku and Svensson, 2019; Zacchello et al., 2017). The components were modelled

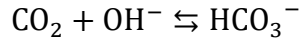
using a True Components Approach that takes into consideration the free and dissociation forms of the components.

2.1 Validation of MEA-CO₂-H₂O Environment in Aspen Plus®

The parameters for the simulation of MEA-CO₂-H₂O environment were adopted from the template ENRTL-RK_RATE_BASED_MEA_MODEL provided by Aspen Plus® for Carbon Capture MEA. The various parameters used in this template (such as Henry's Constants, NRTL constants, Equilibrium constants, and the parameters for reaction kinetics) to define the MEA-H₂O-CO₂ electrolyte system were regressed from experimental data from various sources by the engineers at Aspen Plus® and can be found in the report available with the said template (AspenTech, 2010).

The reaction chemistry for MEA based CO₂ capture consists of three equilibrium reactions and two reversible kinetic reactions (Rxn 1 – 5). The equilibrium constants for all the equilibrium reactions (Rxn 1 – 5) were calculated from the standard Gibbs free energy. The kinetic parameters for the reversible kinetic reactions (Rxn 4 and 5) were obtained from the works of Errico et al. (2016) and tabulated in **Table 1** (Errico et al., 2016). To validate the simulation environment for MEA based CO₂ capture system, a two-stage equilibrium-based absorber was additionally modeled and compared against the pilot plant data (**Table 2**) by Notz et al. (2012).





Rxn 5

Table 1: Kinetic Parameters for Reactions 9 and 10 as obtained from Errico et al. (2016)

	Forward		Reverse	
	$k, \left(\frac{\text{kmol}}{\text{m}^3\text{s}}\right)$	$E_a, \left(\frac{\text{kcal}}{\text{mol}}\right)$	$k, \left(\frac{\text{kmol}}{\text{m}^3\text{s}}\right)$	$E_a, \left(\frac{\text{kcal}}{\text{mol}}\right)$
Rxn. 4	9.77×10^{10}	9.86	3.23×10^{19}	15.65
Rxn. 5	4.32×10^{13}	13.25	2.38×10^{17}	29.45

Table 2: Pilot plant data by Notz et al. (2012)

Parameter	Units	FG ^a	LS ^b
Temperature (T)	°C	48	40
Pressure (P)	bar	1.004	2
Total molar flowrate	kmol/h	2.56	8.74
Mole Fraction			
MEA		0.000	0.103
H ₂ O		0.111	0.869
CO ₂		0.054	0.027
N ₂		0.746	0.00
O ₂		0.089	0.00
Molar CO ₂ Loading	moles CO ₂ /mol MEA	---	0.265

^aFG is Flue Gas inlet stream.

^bLS is Lean Amine inlet stream.

2.2 Simulation of Ionic Liquids in Aspen Plus®

The absorption of CO₂ by AHA-IL is a combination of physisorption as well as chemisorption. While the physisorption is governed by the Henry's constant (Mortazavi-Manesh et al., 2011), chemisorption between AHA-IL and CO₂ occurs as an exothermic reaction via the formation of a reaction intermediate (COOIL) in a 1:1 stoichiometric ratio (Rxn 6).



The ionic liquids, and their corresponding reaction intermediates, were modelled as “pseudocomponents” by specifying the normal boiling points, density, and molecular weights. Additionally, the water solubility and the viscosity data were available from literature for both ILs and were used when specifying the ILs in the Aspen Plus® Properties Environment [23,24,38]. The modelling of the ionic liquids was based on the viscosity (μ) profile, enthalpy of reaction at 40 °C ($\Delta H_{\text{Rxn},40 \text{ °C}}$), and CO₂ absorption capacity (z) profile. A temperature of 40 °C was chosen as the reference as it is the typical operating temperature of a CO₂ absorber (Errico et al. (2016)).

First, the viscosity profile for both the ionic liquids was analyzed. The parameters needed to model the viscosity profile were obtained by regressing the viscosity data into Andrade's temperature dependent equation (Eq 2). As AHA-ILs show no appreciable change in viscosity upon reaction with CO₂, the viscosity of the CO₂-IL reaction intermediate molecules was modelled to be the same as that of their corresponding AHA-ILs.

$$\ln(\mu_i) = A_i + \frac{B_i}{T} + C_i \cdot \ln(T_i) \quad \text{Eq 2}$$

The enthalpy of reaction for both ILs was adjusted by manipulating the heat of formation of the corresponding ionic liquids. The enthalpy of reaction/absorption at a given temperature is theoretically equal to the enthalpy required to cool or heat the reactor divided by the moles of the reactant consumed when both the reactants and the products are maintained at the same temperature. Hence, the heat of the reaction at 40 °C was estimated by running the CSTR isothermally while keeping the temperature of the reactants and the products at 40 °C. The enthalpy of reaction was then adjusted to the desired values, -46.6 kJ/mol of CO₂ for [P2228][2-CNPyrr] and -43.3 kJ/mol of CO₂ for [P2228][2-CNPyrr], by adjusting the heat of formation of the corresponding IL (Gurkan et al., 2010; Song et al., 2019).

The CO₂ absorption profile for the ILs were obtained by running the CSTR adiabatically and regressing the parameters required to fit the temperature dependent equations of the Henry's Law constant, K_H, and the equilibrium constant, K_{eq}, shown in equations 3 and 4, respectively. Additionally, the enthalpy of reaction for the ILs was incorporated into the equilibrium constant by fixing the parameter, B_K. The heat of formation and equilibrium constants are thermodynamically described in Eq 5. The heat of physical absorption was calculated using Eq 6.

$$\ln(K_H) = A_{H,i} + \frac{B_{H,i}}{T} \quad \text{Eq 3}$$

$$\ln(K_{eq}) = A_{K,i} + \frac{B_{K,i}}{T} \quad \text{Eq 4}$$

$$\ln(K_{eq}) = \frac{\Delta S}{R} + \left(\frac{-\Delta H_{chem}^0}{RT} \right) \quad \text{Eq 5}$$

$$\ln(K_H) = \frac{\Delta S}{R} + \left(\frac{-\Delta H_{phy abs}^0}{RT} \right) \quad \text{Eq 6}$$

2.3 Aspen Plus® Simulation Flowsheet

As previously mentioned, the addition of MEA to IL on CO₂ absorption was studied using a CSTR model (**Figure 3**). The inlet streams were specified to be at 1.1 bar and 40 °C, and the reactor was specified to be operating at atmospheric pressure (1.013 bar or 1 atm). The lean solvent consisting of mixture of IL (Stream IL) and non-aqueous MEA (Stream MEA) forms the lean stream (Stream LS) entering the CSTR from the top. The flue gas (Stream CO₂) enters from the bottom, allowing the gaseous CO₂ to counter-currently react with the lean solvent. The CO₂ rich solvent (Stream RS) exits via the bottom, while any unabsorbed vapor stream with low levels of CO₂ exits via the top (Stream Clean Gas).

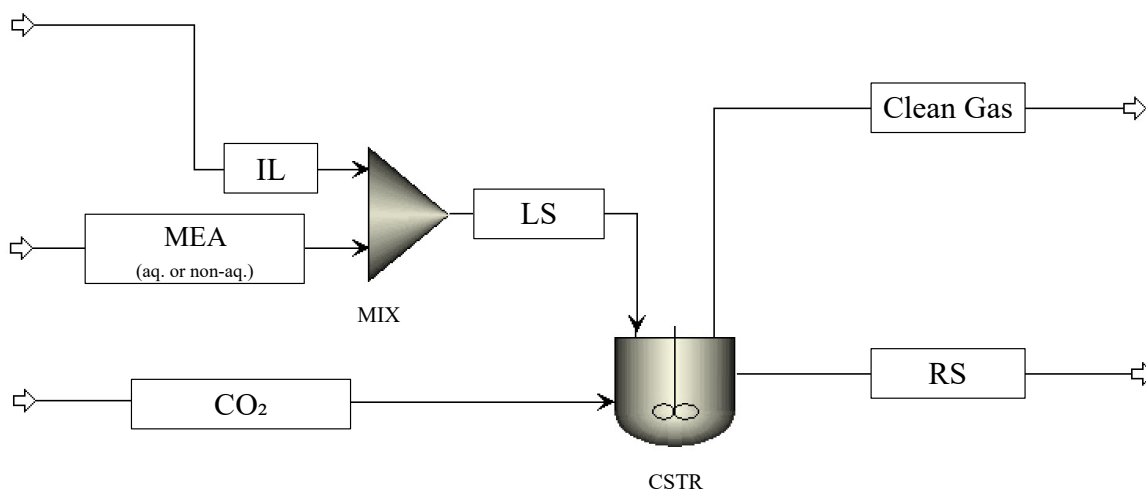


Figure 3: Simulation flowsheet of continuous stirred reactor used to study the effect of addition of aq. and non-aq. MEA to [P2228][2-CNPy] and [P66614][2-CNPy] on CO₂ absorption and viscosity.

2.4 Addition of MEA to Ionic Liquids

The effect of adding MEA to the ILs was studied individually for [P66614][2-CNPy] and [P2228][2-CNPy] using both nonaqueous and 30 wt % aqueous MEA. **Table 3** shows the different hybrid solvent streams considered in this study. A concentration of 30 wt% aqueous MEA was considered in this study as it is the most common amine concentration in industry for CO₂ removal (Barzagli et al., 2016; Brigman et al., 2014; Cebucean et al., 2014; Hamborg et al., 2014; Lv et al., 2015; Matin and Flanagan, 2022; Mores et al., 2012; Morken et al., 2014; Naveiro et al., 2022). Additionally, the effect of CO₂ loaded aqueous MEA streams on the ILs was also considered in this study using a CO₂ loading of 0.3 mol CO₂/mol MEA.

Initially, an equimolar ratio of ionic liquid to CO₂ gas stream was specified as inlets to the CSTR. MEA was then added in increments of 0.5 mol % to the IL to a maximum of 95 mol % MEA. The CO₂ capture performance of all the four hybrid solvents was then studied systematically. In particular, the effect of the addition of MEA to the ionic liquid was studied by plotting the outlet adiabatic temperature, the diffusivity of CO₂ in the hybrid solvent, the CO₂ absorption capacity (z), and the heat of the reaction of CO₂ and IL at 40 °C (ΔH_{Rxn} at 40 °C). While the first two parameters were directly obtained from the Aspen Plus[®] simulation, the latter two parameters were calculated as shown below.

$$CO_2 \text{ Absorption Capacity } (z) = \frac{n_{ILCOO} + n_{CO_2 \text{ phy.abs}} + n_{MEACOO}}{n_{IL,in} + n_{MEA,in}} \quad \text{Eq 7}$$

$$\text{Enthalpy of Reaction at 40 °C } (\Delta H_{Rxn \text{ at } 40 \text{ °C}}) = \frac{\text{Duty of Reactor (at 40 °C)}}{n_{CO_2,in} \text{ (Total)}} \quad \text{Eq 8}$$

where,

n_{ILCOO} = number of moles of ILCOO intermediated formed after reaction of CO₂ with IL

$n_{CO_2 phy.abs}$ = number of moles of CO₂ physically absorbed into the solvent without conversion

n_{MEACOO^-} = number of moles of MEACOO⁻ intermediated formed after reaction of CO₂ with MEA

$n_{IL,in}$ = number of moles of IL input

$n_{MEA,in}$ = number of moles of MEA input

Duty of Reactor (at 40 °C) = Heat released by the reactor when the temperature of the reaction products is reduced from their adiabatic temperature to 40 °C.

$n_{CO_2,in (Total)}$ = Total number of moles of CO₂ inlet into the reactor through the gas stream.

When CO₂ loaded aq. MEA is used as a cosolvent,

$n_{CO_2,in (Total)}$ = sum of the total CO₂ in through the flue gas stream and the number of moles CO₂ present in the CO₂ loaded aqueous MEA stream

Hybrid solvents suitable for CO₂ capture were then identified based on the study. The composition of the suggested hybrid solvents was then selected such that the viscosity of the hybrid solvent was reduced compared to pure IL and the enthalpy of reaction of the hybrid solvent was reduced when compared to that of MEA.

Table 3: Experimental Design

Name of Hybrid Solvent	[P2228]	[P66614]	Nonaqueous MEA	30% Aqueous MEA	
	[2-CNPyr]	[2-CNPyr]		w/o CO ₂ Loading	w/ CO ₂ Loading
A1	✓		✓		
A2 w/o CO ₂ Loading	✓			✓	
A2 w/ CO ₂ Loading	✓				✓
B1		✓	✓		
B2 w/o CO ₂ Loading		✓		✓	
B2 w/ CO ₂ Loading		✓			✓

3. Results and Discussions

3.1 MEA Environment Validation

The environment for CO₂ capture using aqueous MEA was validated by comparing the results of a CO₂ capture absorber (**Figure 4**) simulated in Aspen Plus[®] to that of the pilot plant

described by Notz et al. (2012). Typically, an absorber for CO₂ Capture in Aspen Plus® can be simulated either in a Rate Based Mode that allows the user to consider the limitations to mass transfer in the presence of a chemical reaction (Madeddu et al., 2019), or, in an Equilibrium Based mode by introducing the Murphree tray efficiency parameter (Øi, 2012).

In this study, a two-stage equilibrium-based approach was satisfactory as the percent error between the Pilot Plant and the simulation was minimal. Therefore, an equilibrium-based approach was an acceptable approximation. **Table 4** shows the experimental and simulated results of CO₂ capture around the absorber as well as the corresponding error in the CO₂ rich amine stream (RS) leaving the absorber.

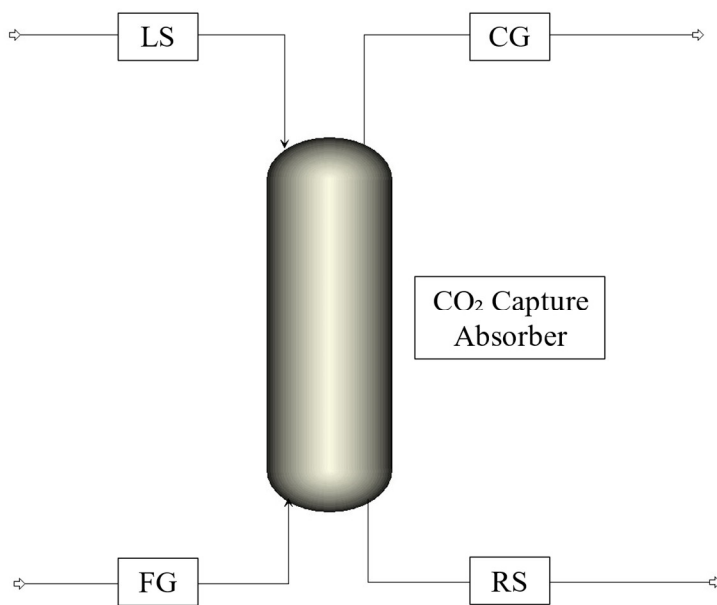


Figure 4: Aspen Plus® Simulation of 2-Stage Equilibrium absorber used to verify the aqueous MEA environment. FG, LA, CG and RS represent the Flue Gas inlet, Lean Amine inlet, Clean Gas outlet and Rich Amine stream.

Table 4: Comparison of Rich Amine Stream (RS) determined by simulation versus pilot plant data.

Parameter	Value	Experimental [Notz et al. (2012)]	Simulation	Error %
Temperature (T)	°C	51.66	51.28	-0.74%
Pressure (P)	bar	1.065	1.065	--
Total molar flowrate	kmol/hr	8.82	9.02	2.27%
Mole Fraction				
MEA		0.102	0.1	-0.98%
H ₂ O		0.859	0.858	-0.12%
CO ₂		0.039	0.041	5.13%
N ₂		0	0	--
O ₂		0	0	--
Molar CO ₂ Loading		0.387	0.419	8.27%

3.2 Validation of AHA-ILs

The experimental data (Gurkan et al., 2010; Song et al., 2019) for viscosity and CO₂ absorption of both the ILs were modelled using Aspen Plus® (**Figure 5**). The enthalpy of reaction ($\Delta H_{\text{Chem.}}$) and enthalpy of dissolution ($\Delta H_{\text{Phy.}}$) for both the two ILs are shown in **Table 5** and are in good agreement with the values found in literature. The high R² values of the viscosity and CO₂ absorption profiles for both the ILs are indicative of adequate modelling of ILs and their reaction intermediates within the simulation. The R² values for the viscosity and CO₂ Absorption Profile along with their corresponding fitting parameters for both the AHA-ILs can be found in Supplementary Document A (**Table S1** and **Table S2**, respectively).

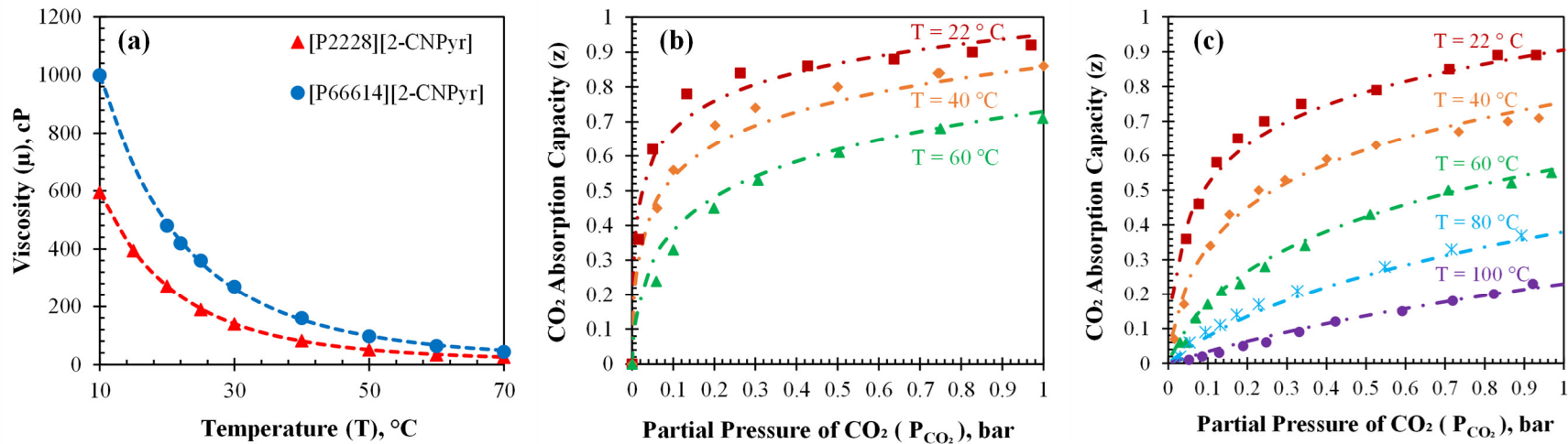


Figure 5: Ionic Liquid Validation: a) Viscosity profile of ionic liquids vs Experimental Data; b) CO₂ Absorption Profile vs Experimental Data for [P2228][2-CNPyrr]; and c) CO₂ Absorption Profile vs Experimental Data for [P66614][2-CNPyrr]. The markers represent experimental data from literature (Gurkan et al., 2010; Song et al., 2019). The dotted lines represent the CO₂ absorption profiles obtained from the simulation.

Table 5: Validation Results of [P2228][2-CNPyrr] & [P66614][2-CNPyrr]

Parameters	Units	[P2228][2-CNPyrr]		[P66614][2-CNPyrr]	
		Chem.	Phy.	Chem.	Phy.
Change in Entropy (ΔS)	$\frac{J}{mol \cdot K}$	-90.99	-151.94	-97.57	-158.23
Change in Enthalpy (ΔH)	$\frac{kJ}{mol}$	-46.60	-11.04	-43	-13.20

3.3 Effect of nonaqueous MEA on Viscosity and CO₂ Absorption Capacity of IL

The effect of aqueous and nonaqueous MEA on the viscosity of [P2228][2-CNPyrr] & [P66614][2-CNPyrr] can be seen in **Figure 5**. In this graph, Solvent A1 and Solvent B1 depicts the dilution of IL with non-aqueous MEA. Solvent A2 and B2 (with or without CO₂ loading) pertain to the dilution of the corresponding ILs with aqueous MEA with or without CO₂ loading, respectively. **Figure 6** shows that the addition of MEA to the ILs exhibits a decrease in the viscosity of the solvent as was expected. The viscosity of the hybrid solvents formed by diluting AHA-IL with nonaqueous MEA was lower than hybrid solvents formed by the diluting AHA-ILs with aqueous MEA.

CO₂ loading shows no considerable effect on the viscosity of the hybrid solvent A2 at lower concentrations of aqueous MEA. However, at concentrations > 25 mol % aqueous MEA in the IL, the viscosity of solvent A2 with CO₂ loading is slightly higher than that without CO₂ loading. This increase in the viscosity of the hybrid solvent at higher concentrations of MEA can be ascribed to MEA which exhibits a subtle increase in the viscosity upon CO₂ absorption (Perumal et al., 2020; Zhang et al., 2015).

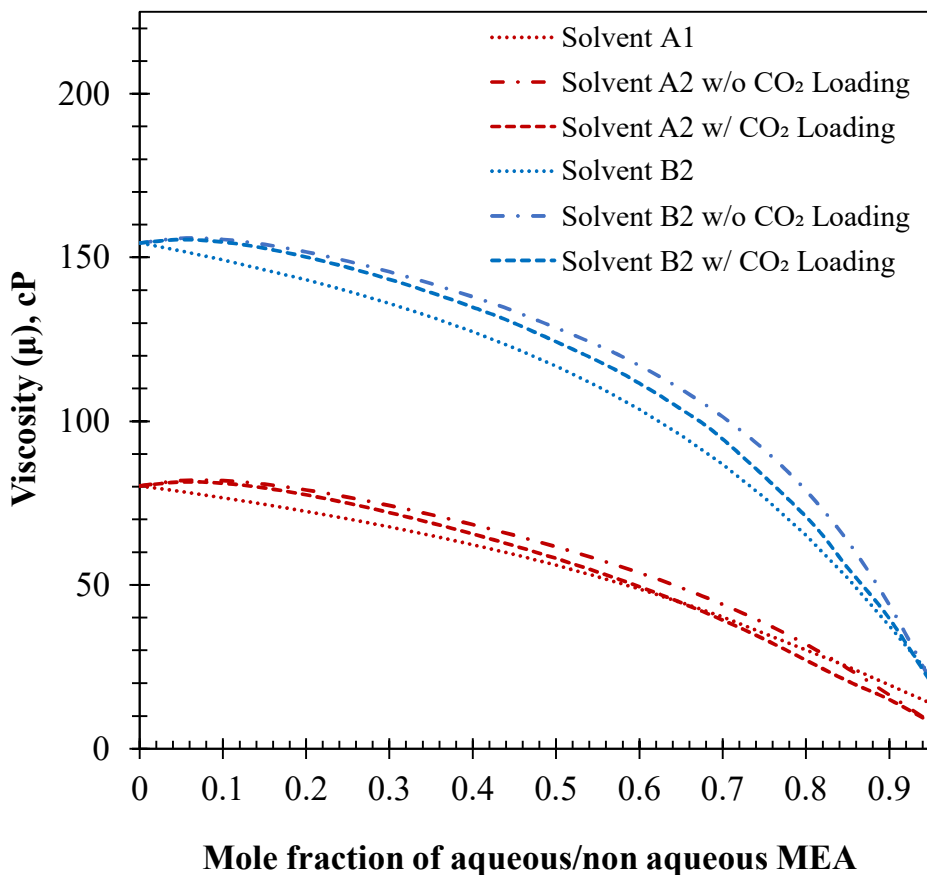


Figure 6: Viscosity profiles for various hybrid solvents. The inlet streams were specified at 40°C and 1.1 bar. The CSTR was operated adiabatically at a pressure of 1.013 bar or 1 atm.

The effect of nonaqueous MEA on CO₂ absorption capacity (z) is shown in **Figure 7**. For the hybrid solvents made from nonaqueous MEA and AHA-IL, it is observed that both the AHA-ILs exhibit a near linear reduction in the CO₂ capture capacity of the hybrid solvent. This trend continues to ~50 mol % MEA. This reduction in the CO₂ absorption capacity can be attributed to the dilution of the IL with MEA. Additionally, the increase of CO₂ absorption capacity (z) beyond ~50 mol % MEA and until ~70 mol % can be attributed to the changing diffusivity of CO₂ (**Figure 8c**). As the diffusivity of CO₂ in the solvent increases, the reactivity (enthalpy of reaction) increases, thereby increasing the outlet temperature (**Figure 8a**). The increase in the

outlet temperature is a result of the combined exothermic reactions of the IL and MEA with CO₂ (as shown in **Figure 8b**). This increase in temperature shifts the equilibrium towards the reactants, thereby decreasing the CO₂ absorption beyond the 70 mol % mark.

Figure 8a also shows that the mean adiabatic temperature of the outlet streams reaches temperatures ≥ 100 °C, which is due to the exothermic reactions between CO₂, MEA, and IL. These temperatures are close to the thermal degradation temperatures of MEA. Hence, Solvents A1 and B1 cannot be recommended for utilization in CO₂ capture process equipment as they increase the risk of MEA degradation.

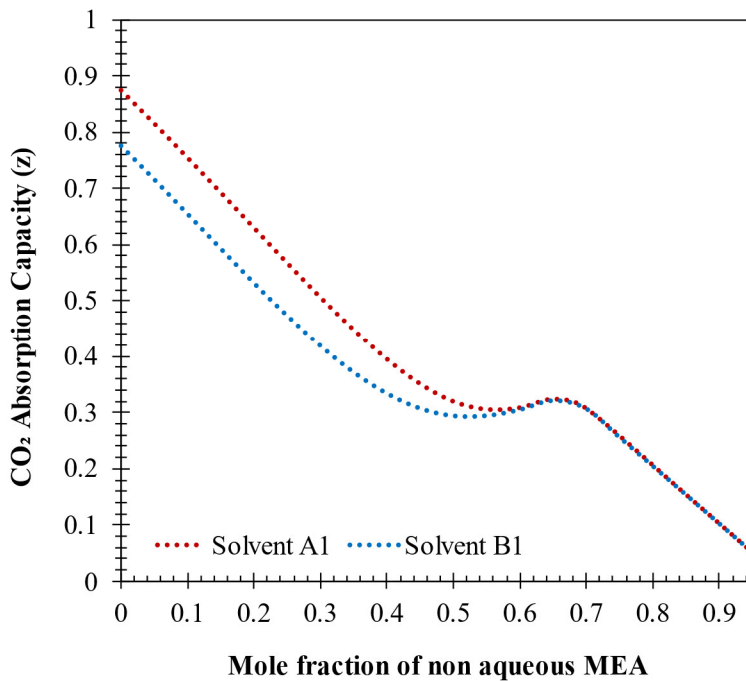


Figure 7: CO₂ Capture Capacity (z) v/s Mole Fraction of MEA in IL for hybrid solvents A1 and B1. The inlet streams were specified at 40°C and 1.1 bar. The CSTR was operated adiabatically at a pressure of 1.013 bar.

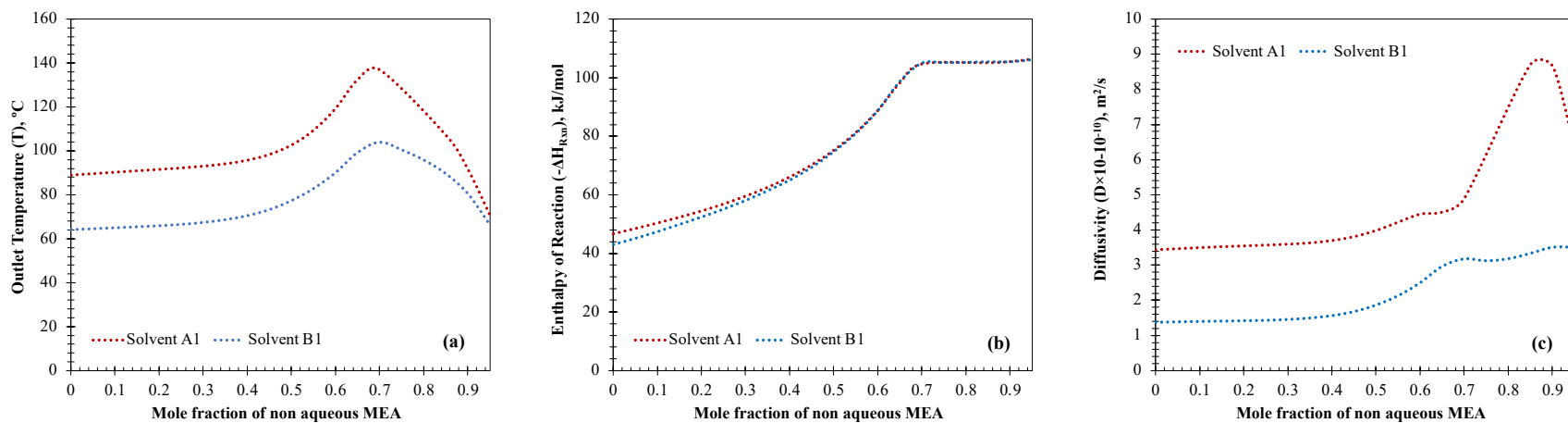


Figure 8: (a) Outlet temperature, (b) Enthalpy of reaction ($-\Delta H_{Rxn}$), (c) Diffusivity of CO_2 in hybrid solvent during CO_2 capture vs mole fraction MEA in hybrid solvent. The inlet streams were specified at $40^\circ C$ and 1.1 bar. The CSTR was operated adiabatically at a pressure of 1.013 bar or 1 atm.

3.4 Effect of aqueous MEA on Viscosity and CO₂ Absorption Capacity of IL

Figure 9a shows the variation in CO₂ capture capacity (z) of the two hybrid solvents with increasing aqueous MEA concentration at two different CO₂ loadings of aqueous MEA. As can be immediately noticed, CO₂ loading of the aqueous MEA does not contribute to the overall CO₂ capture capacity of the hybrid solvent. The CO₂ capture capacity of both the solvents exhibit an overall decrease in z with an increase in the concentration of aqueous MEA due to dilution. It can also be noted that z of the hybrid solvent initially exhibits an increase in the capture capacity to ~ 20 mol % of aqueous MEA. This change can prominently be seen in Solvent B2 (as opposed to Solvent A2) because the inherent CO₂ capture ability of [P66614] is lower than that of [P2228], thereby allowing the IL to have a significant rise in z when mixed with aqueous MEA.

The variation of z can also be explained by plotting the diffusivity of CO₂ in the solvent against the concentration of MEA in the Hybrid solvent (**Figure 9b**). The addition of aqueous MEA to the IL initially reduces the amount of CO₂ that diffuses into the liquid, causing an initial decrease in the z of the hybrid solvent. However, between 12 and 25 mol % of aqueous MEA, the diffusivity increases, thereby increasing the CO₂ absorption capacity of the hybrid solvent. Beyond 25 mol %, the diffusivity and the absorption capacity reduce due to dilution. This decrease is noticed until 75 mol % of MEA, after which the diffusivity of CO₂ increases exponentially as the viscosity of the solvent also falls dramatically. This phenomenon can also be seen in the CO₂ absorption capacity.

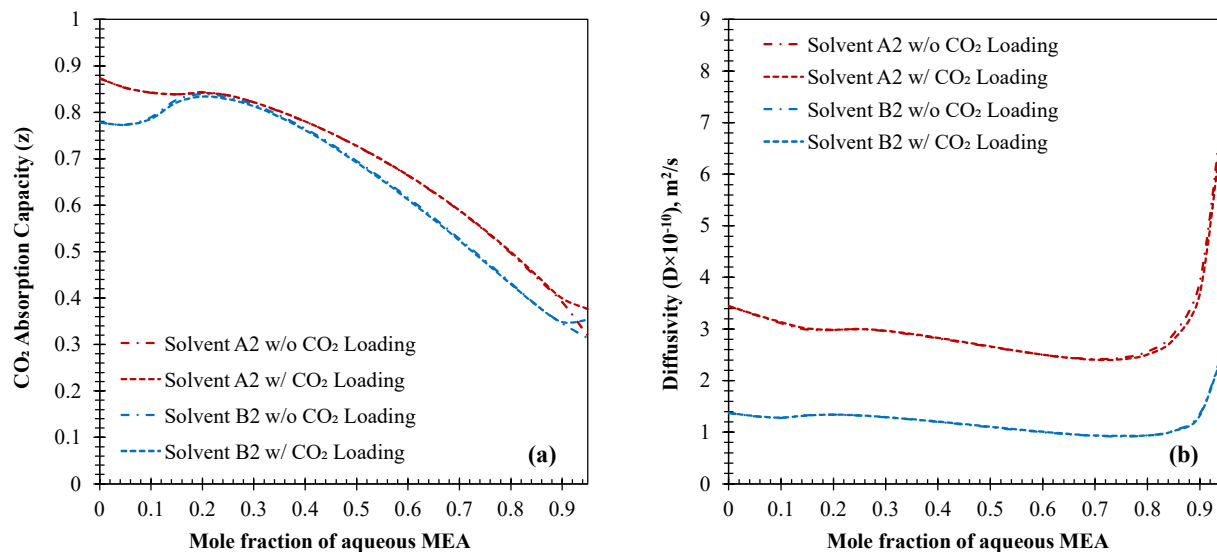


Figure 9: (a) CO₂ Absorption Capacity (z) of the hybrid solvent, and (b) Diffusivity of CO₂ in hybrid solvent during CO₂ capture as function of mole fraction of aqueous MEA in hybrid solvents A2 and B2. The inlet streams were specified at 40°C and 1.1 bar. The CSTR was operated adiabatically at a pressure of 1.013 bar or 1 atm.

Additionally, the adiabatic increase in temperature of the outlet stream (**Figure 10a**) also correlates with the diffusivity of CO₂ in the hybrid solvent. A reduction in the diffusivity reduces the temperature as there is less CO₂ available to react. However, the overall enthalpy of reaction (**Figure 10b**) increases linearly up to ~ 60 mol% of aqueous MEA) in IL, beyond which the increase is exponential. It can be noticed that the slope of the exponential increase is steeper for the hybrid solvents without CO₂ loading than the solvents with CO₂ Loading. This difference in the slope might be attributed to the depletion of CO₂ in non-CO₂ loaded solvents.

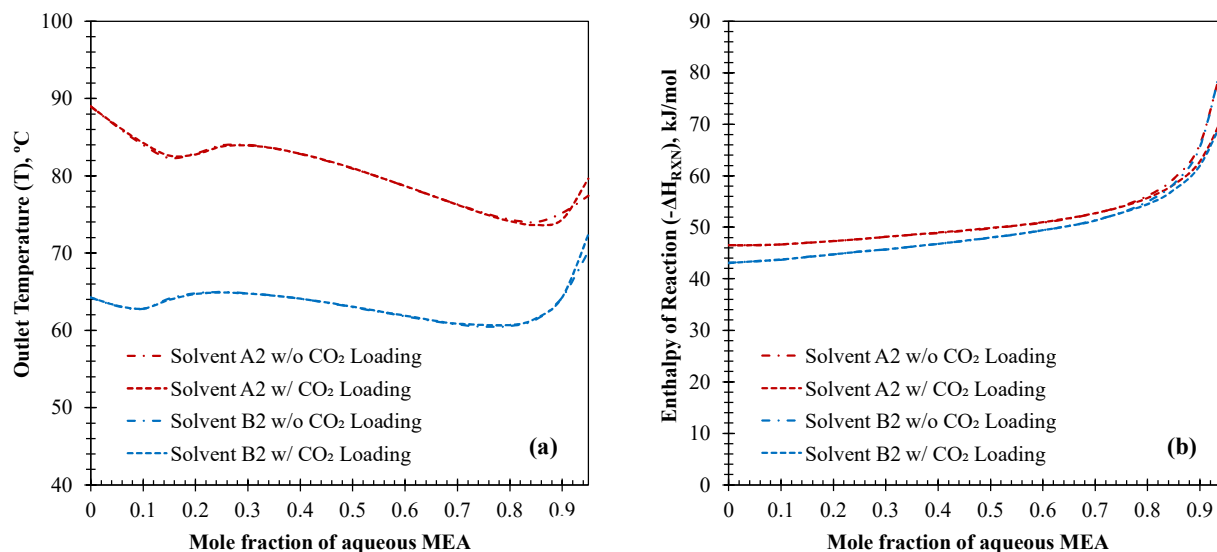


Figure 10: (a) Mean temperature of the outlet streams, and (b) Enthalpy of reaction during CO₂ capture as function of mole fraction aqueous MEA in hybrid solvents A2 and B2. The inlet streams were specified at 40°C and 1.1 bar. The CSTR was operated adiabatically at a pressure of 1.013 bar or 1 atm.

3.5 Composition Selection

Based on the results in the previous sections, solvents A1 and B1 were eliminated from this section. The results from Section 3.4 also indicate that the addition of aqueous MEA with CO₂ loading to IL had no significant difference in the behavior of solvents A2 and B2. Hence, only the hybrid solvents made from IL and aqueous MEA without CO₂ loading were used to select a composition of the hybrid solvent that is less exothermic than MEA and has a lower viscosity than its constituent IL.

A sensitivity analysis was performed comparing the enthalpy of reaction (at 40 °C) and the viscosity for various concentrations of 30 wt% aqueous MEA in both the ionic liquids. The

values obtained from the sensitivity analysis were equally weighted and normalized between 0 and 1 to bring both the parameters to the same scale (**Eq 9**). The point of intersection of the normalized viscosity and enthalpy of reaction parameters would then be the desired point for the hybrid solvents as shown in **Figure 11**. The corresponding values for the enthalpy of reaction, viscosity, and composition of the hybrid solvents are found in **Table 6**.

$$\text{Normalized Value} = \frac{(x-x_{\min})}{(x_{\max}-x_{\min})} \quad \text{Eq 9}$$

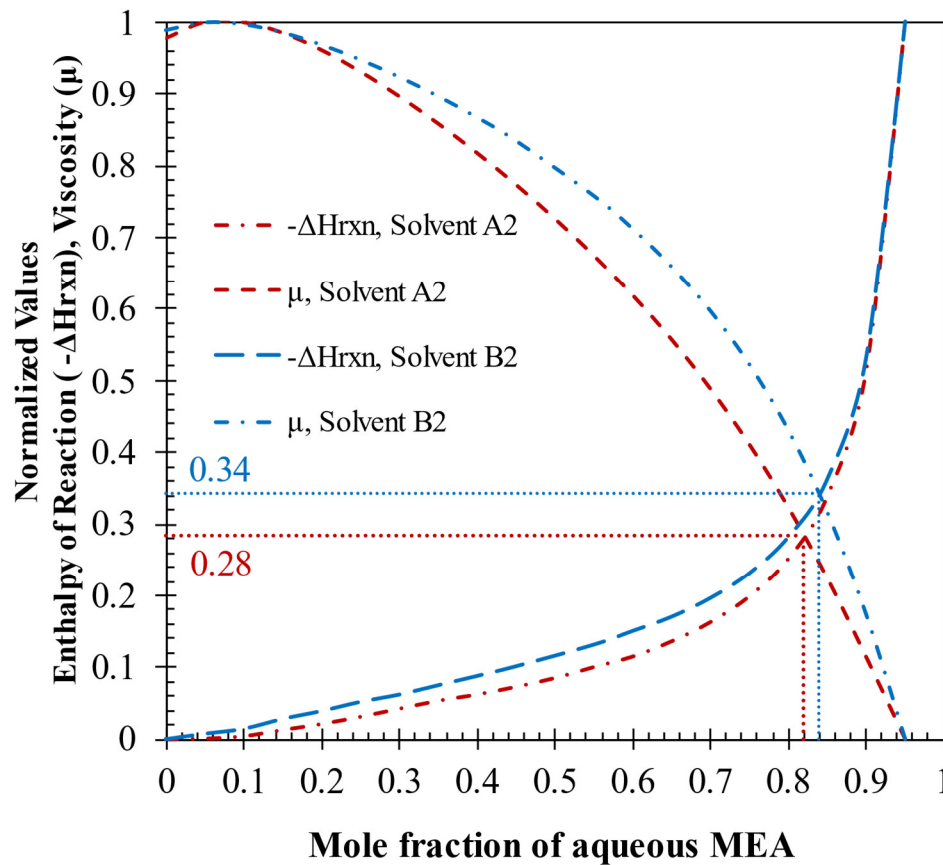


Figure 11: Normalized enthalpy of reaction ($-\Delta H_{Rxn}$) and Viscosity v/s mole fraction of aqueous MEA in IL for hybrid solvents A2 and B2. The inlet streams were specified at 40°C and 1.1 bar. The CSTR was operated adiabatically at a pressure of 1.013 bar.

Table 6: Results of composition selection of the hybrid solvents A2 and B2

Parameters	Units	Solvent A2	Solvent B2
Enthalpy of reaction (at 40 °C), $\Delta H_{Rxn, 40\text{ }^\circ\text{C}}$	kJ/mol	-57.38	-57.61
Viscosity, μ	cP	29.06	67.04
$X_{\text{aqueous MEA}}^a$		0.8192	0.8381
X_{IL}^a		0.1808	0.1619

^ax is component mole fraction.

The results illustrate that Solvent A2 and Solvent B2 exhibit comparable enthalpy of reaction at ~ 57 kJ/mol of CO₂ absorbed, which is approximately 32% lower than that of conventional aqueous MEA solvents. The marginally lower reaction enthalpy of the hybrid solvent B2 can be attributed to the slightly lower enthalpy of reaction of its corresponding IL i.e. [P66614][2-CNPy], -43 kJ/mol v/s -46.6 kJ/mol for [P2228][2-CNPy].

Solvent A2, however, is a better hybrid solvent for CO₂ capture because, in addition to having a comparable enthalpy of reaction at 40°C to that of Solvent B2), this solvent also exhibits a lower viscosity compared to Solvent B2. The lower viscosity of Solvent A2 can be attributed to the lower viscosity of its constituent ionic liquid. i.e [P2228][2-CNPy] compared to [P66614][2-CNPy].

Additionally, the results obtained in this study were also comparable to the results obtained by Yang et al. (2014) in which a hybrid solvent of 0.3:0.4:0.3 w/w/w of MEA/[bmim][BF₄]/H₂O exhibited a reduction in the regeneration energy of ~ 37 % for mixture compared to that of traditional aqueous amine-based CO₂ capture. A representative Input Summary Files for Solvent

A1 and Solvent A2 (w and w/o CO₂ Loading) can be found in Appendix 1, 2 and 3 of Supplementary Document B.

4. Conclusion

This work presents a simulation model study on the effect of nonaqueous and aqueous monoethanolamine (MEA) on phosphonium based Aprotic Heterocyclic Anion type ionic liquids (AHA-ILs), Triethyloctylphosphonium 2-cyanopyrrolide, [P2228][2-CN₂Pyr], and Trihexyltetradecylphosphonium 2-cyanopyrrolide, [P66614][2-CN₂Pyr]. Hybrid solvents were formed by diluting each IL with nonaqueous MEA and 30 wt % aqueous MEA. Various concentrations of these hybrid solvents were evaluated to study their effect on the CO₂ absorption capacity and the viscosity of the ILs. Although ILs have approximately 47% lower enthalpy of reaction compared to MEA, the solvent most currently used for CO₂ capture, they also possess higher viscosity, hindering the diffusivity of CO₂ into the absorbing solvent.

This study found that all hybrid solvents exhibited an overall improvement in CO₂ absorption by reducing the viscosity compared to using IL as the sole absorption fluid. Solvent mixtures of IL and nonaqueous MEA resulted in outlet stream temperatures exceeding the degradation temperature of MEA (> 120°C) due to the exothermic nature of the reactions between AHA-IL, MEA, and CO₂. Solvents consisting of aqueous MEA, however, did not have this issue. Water in the hybrid solvent functioned as a coolant to absorb the heat of the reactions. Therefore, water plays a vital role in managing the temperature of the absorber when utilizing MEA as a co-solvent with AHA-ILs.

Of the mixtures studied, only the hybrid solvent made from ILs and 30 wt % aqueous MEA are recommended for carbon capture operations. The compositions of the hybrid solvents

obtained based on the selection criteria exhibited reduced viscosity (compared to pure ILs) and enthalpy of reaction (compared to MEA). [P2228][2-CNPyrr]/ 30 wt% aqueous MEA was determined to be the best solvent with $\Delta H_{\text{Rxn}} = -57.38$ kJ/mol of CO₂ absorbed, (32% lower than aqueous MEA) and a viscosity of 29.06 cP that is 64% lower than pure [P2228][2-CNPyrr].

The favorable performance of [P2228][2-CNPyrr]/ 30 wt% aqueous MEA based hybrid solvent in this study highlights a promising future for AHA-IL and aqueous MEA hybrid solvents in the field of carbon capture. This study shows that hybrid solvents of such kind would not only possess the potential to address the challenge of the high viscosity often associated with the ILs but also exhibit improved CO₂ absorption capacity compared to MEA and maintain a feasible CO₂ absorption temperature that is practical and suitable for industrial CO₂ capture applications. This study also serves as a groundwork for future endeavors at optimizing and implementing similar hybrid solvents for various CO₂ capture applications.

Declaration of Competing Interests

The authors declare no competing financial interest.

Acknowledgment

This material is based upon work supported by the Department of Energy under DOE Award Number DE-FE0031558.

Disclaimer: This report was prepared as an account of work sponsored by an agency of the United States Government. Neither the United States Government nor any agency thereof, nor any of their employees, makes any warranty, express or implied, or assumes any legal liability or responsibility for the accuracy, completeness, or usefulness of any information, apparatus,

product, or process disclosed, or represents that its use would not infringe privately owned rights. Reference herein to any specific commercial product, process, or service by trade name, trademark, manufacturer, or otherwise does not necessarily constitute or imply its endorsement, recommendation, or favoring by the United States Government or any agency thereof. The views and opinions of authors expressed herein do not necessarily state or reflect those of the United States Government or any agency thereof.

References

- Akinola, T.E., Oko, E., Wang, M., 2019. Study of CO₂ removal in natural gas process using mixture of ionic liquid and MEA through process simulation. *Fuel* 236, 135–146.
<https://doi.org/10.1016/j.fuel.2018.08.152>
- American Chemical Society, 2013. Changes since the industrial revolution.
<https://www.acs.org/content/acs/en/climatescience/greenhousegases/industrialrevolution.html> (accessed 15 February 2022).
- Anderson, J.L., Dixon, J.K., Brennecke, J.F., 2007. Solubility of CO₂, CH₄, C₂H₆, C₂H₄, O₂, and N₂ in 1-hexyl-3-methylpyridinium bis(trifluoromethylsulfonyl)imide: Comparison to other ionic liquids. *Acc. Chem. Res.* 40, 1208–1216. <https://doi.org/10.1021/ar7001649>
- AspenTech, 2019. Aspen Physical Property System – Physical Property Models.
- AspenTech, 2010. Aspen Plus: Rate-based model of the CO₂ capture process by MEA using Aspen Plus (ENRTL-RK) 1–25.
- Avelar Bonilla, G.M., Morales-Collazo, O., Brennecke, J.F., 2019. Effect of water on CO₂ capture by aprotic heterocyclic anion (AHA) ionic liquids. *ACS Sustain. Chem. Eng.* 7, 16858–16869. <https://doi.org/10.1021/acssuschemeng.9b04424>
- Baj, S., Siewniak, A., Chrobok, A., Krawczyk, T., Sobolewski, A., 2013. Monoethanolamine and ionic liquid aqueous solutions as effective systems for CO₂ capture. *J. Chem. Technol. & Biotechnol.* 88, 1220–1227. <https://doi.org/10.1002/jctb.3958>
- Barzagli, F., Mani, F., Peruzzini, M., 2016. A comparative study of the CO₂ absorption in some solvent-free alkanolamines and in aqueous monoethanolamine (MEA). *Environ. Sci. Technol.* 50, 7239–7246. <https://doi.org/10.1021/acs.est.6b00150>

- Brennecke, J.F., Gurkan, B.E., 2010. Ionic liquids for CO₂ capture and emission reduction. *J Phys. Chem. Lett.* 1, 3459–3464. <https://doi.org/10.1021/jz1014828>
- Brigman, N., Shah, M.I., Falk-Pedersen, O., Cents, T., Smith, V., De Cazenove, T., Morken, A.K., Hvidsten, O.A., Chhaganlal, M., Feste, J.K., Lombardo, G., Bade, O.M., Knudsen, J., Subramoney, S.C., Fostås, B.F., De Koeijer, G., Hamborg, E.S., 2014. Results of amine plant operations from 30 wt% and 40 wt% aqueous MEA testing at the CO₂ Technology Centre Mongstad. *Energy Procedia* 63, 6012–6022. <https://doi.org/10.1016/j.egypro.2014.11.635>
- Cebucean, D., Cebucean, V., Ionel, I., 2014. CO₂ capture and storage from fossil fuel power plants. *Energy Procedia* 63, 18–26. <https://doi.org/10.1016/j.egypro.2014.11.003>
- Davis, J., Rochelle, G., 2009. Thermal degradation of monoethanolamine at stripper conditions. *Energy Procedia* 1, 327–333. <https://doi.org/10.1016/j.egypro.2009.01.045>
- de Riva, J., Ferro, V., Moya, C., Stadtherr, M.A., Brennecke, J.F., Palomar, J., 2018. Aspen Plus supported analysis of the post-combustion CO₂ capture by chemical absorption using the [P2228][CNPyr] and [P66614][CNPyr] AHA ionic liquids. *Int. J. Greenh. Gas Control* 78, 94–102. <https://doi.org/10.1016/j.ijggc.2018.07.016>
- Deyab, M.A., Mohsen, Q., 2021. Impact of phosphonium-based ionic liquid on the corrosion control of aluminum alloy AA5052 in MED desalination plants during acid cleaning process. *J. Mol. Liq.* 334, 116121. <https://doi.org/10.1016/j.molliq.2021.116121>
- Errico, M., Madeddu, C., Pinna, D., Baratti, R., 2016. Model calibration for the carbon dioxide-amine absorption system. *Appl. Energy* 183, 958–968. <https://doi.org/10.1016/j.apenergy.2016.09.036>

- Fredriksen, S.B., Jens, K.J., 2013. Oxidative degradation of aqueous amine solutions of MEA, AMP, MDEA, Pz: A review. *Energy Procedia* 37, 1770–1777.
<https://doi.org/10.1016/j.egypro.2013.06.053>
- Garip, M., Gizli, N., 2020. Ionic liquid containing amine-based silica aerogels for CO₂ capture by fixed bed adsorption. *J. Mol. Liq.* 310, 113227.
<https://doi.org/https://doi.org/10.1016/j.molliq.2020.113227>
- Gurjar, S., Sharma, S.K., Sharma, A., Ratnani, S., 2021. Performance of imidazolium based ionic liquids as corrosion inhibitors in acidic medium: A review. *Appl. Surf. Sci. Adv.* 6, 100170.
<https://doi.org/10.1016/j.apsadv.2021.100170>
- Gurkan, B., Goodrich, B.F., Mindrup, E.M., Ficke, L.E., Massel, M., Seo, S., Senftle, T.P., Wu, H., Glaser, M.F., Shah, J.K., Maginn, E.J., Brennecke, J.F., Schneider, W.F., 2010. Molecular design of high capacity, low viscosity, chemically tunable ionic liquids for CO₂ capture. *J. Phys. Chem. Letters* 1, 3494–3499. <https://doi.org/10.1021/jz101533k>
- Hamborg, E.S., Smith, V., Cents, T., Brigman, N., Falk-Pedersen, O., De Cazenove, T., Chhaganlal, M., Feste, J.K., Ullestad, Ø., Ulvatn, H., Gorset, O., Askestad, I., Gram, L.K., Fostås, B.F., Shah, M.I., Maxson, A., Thimsen, D., 2014. Results from MEA testing at the CO₂ Technology Centre Mongstad. Part II: Verification of baseline results. *Energy Procedia* 63, 5994–6011. <https://doi.org/10.1016/j.egypro.2014.11.634>
- Hospital-Benito, D., Lemus, J., Moya, C., Santiago, R., Ferro, V.R., Palomar, J., 2021. Techno-economic feasibility of ionic liquids-based CO₂ chemical capture processes. *Chem. Eng. J.* 407, 127196. <https://doi.org/10.1016/j.cej.2020.127196>

- Hospital-Benito, D., Lemus, J., Moya, C., Santiago, R., Palomar, J., 2020. Process analysis overview of ionic liquids on CO₂ chemical capture. *Chem. Eng. J.* 390, 124509.
<https://doi.org/10.1016/j.cej.2020.124509>
- Kaya, S., Erkan, S., Simşek, S., Kumar, A., 2021. Ionic liquids as corrosion inhibitors. *ACS Symp. Ser.* 1404, 103–119. <https://doi.org/10.1021/BK-2021-1404.CH004>
- Lei, Z., Chen, B., Koo, Y.M., Macfarlane, D.R., 2017. Introduction: Ionic liquids. *Chem. Rev.* 10,6633–6635. <https://doi.org/10.1021/acs.chemrev.7b00246>
- Lian, S., Song, C., Liu, Q., Duan, E., Ren, H., Kitamura, Y., 2021. Recent advances in ionic liquids-based hybrid processes for CO₂ capture and utilization. *J. Environ. Sci.* 99, 281–295.
<https://doi.org/https://doi.org/10.1016/j.jes.2020.06.034>
- Luis, P., 2016. Use of monoethanolamine (MEA) for CO₂ capture in a global scenario: Consequences and alternatives. *Desalination* 380, 93–99.
<https://doi.org/10.1016/j.desal.2015.08.004>
- Ly, B., Guo, B., Zhou, Z., Jing, G., 2015. Mechanisms of CO₂ capture into monoethanolamine solution with different CO₂ loading during the absorption/desorption processes. *Environ. Sci Technol.* 49, 10728–10735. <https://doi.org/10.1021/acs.est.5b02356>
- Madeddu, C., Errico, M., Baratti, R., 2019. CO₂ Capture by Reactive Absorption-Stripping, *Springer Briefs in Energy*. Springer International Publishing, Cham.
<https://doi.org/10.1007/978-3-030-04579-1>
- Madugula, A. C. S., Sachde, D., Hovorka, S. D., Meckel, T. A., & Benson, T. J. (2021). Estimation of CO₂ emissions from petroleum refineries based on the total operable capacity for carbon capture applications. *Chemical Engineering Journal Advances*, 8, 100162.
<https://doi.org/10.1016/j.cej.2021.100162>

- Maham, Y., Liew, C.N., Mather, A.E., 2002. Viscosities and excess properties of aqueous solutions of ethanolamines from 25 to 80°C. *J. Solut. Chem.* 31, 743–756.
<https://doi.org/10.1023/a:1021133008053>
- Matin, N. S., Flanagan, W.P., 2022. Life cycle assessment of amine-based versus ammonia-based post combustion CO₂ capture in coal-fired power plants. *Int. J. Greenh. Gas Control* 113, 103535. <https://doi.org/10.1016/j.ijggc.2021.103535>
- Mores, P., Scenna, N., Mussati, S., 2012. CO₂ capture using monoethanolamine (MEA) aqueous solution: Modeling and optimization of the solvent regeneration and CO₂ desorption process. *Energy* 45, 1042–1058. <https://doi.org/10.1016/j.energy.2012.06.038>
- Morken, A.K., Nenseter, B., Pedersen, S., Chhaganlal, M., Feste, J.K., Tyborgnes, R.B., Ullestad, Ø., Ulvatn, H., Zhu, L., Mikoviny, T., Wisthaler, A., Cents, T., Bade, O.M., Knudsen, J., De Koeijer, G., Falk-Pedersen, O., Hamborg, E.S., 2014. Emission results of amine plant operations from MEA testing at the CO₂ Technology Centre Mongstad. *Energy Procedia* 63, 6023–6038. <https://doi.org/10.1016/j.egypro.2014.11.636>
- Mortazavi-Manesh, S., Satyro, M., Marriott, R.A., 2011. A semi-empirical Henry's law expression for carbon dioxide dissolution in ionic liquids. *Fluid Phase Equilib* 307, 208–215. <https://doi.org/10.1016/j.fluid.2011.05.006>
- Naveiro, M., Romero Gómez, M., Arias-Fernández, I., Baaliña Insua, Á., 2022. Thermodynamic and environmental analyses of a novel closed loop regasification system integrating ORC and CO₂ capture in floating storage regasification units. *Energy Convers. Manag.* 257, 115410. <https://doi.org/10.1016/j.enconman.2022.115410>

- Nittaya, T., Douglas, P.L., Croiset, E., Ricardez-Sandoval, L.A., 2014. Dynamic modeling and evaluation of an industrial-scale CO₂ capture plant using monoethanolamine absorption processes. *Ind. Eng. Chem. Res* 53, 11411–11426. <https://doi.org/10.1021/ie500190p>
- Notz, R., Mangalapally, H.P., Hasse, H., 2012. Post combustion CO₂ capture by reactive absorption: Pilot plant description and results of systematic studies with MEA. *International J. Greenh. Gas Control* 6, 84–112. <https://doi.org/10.1016/J.IJGGC.2011.11.004>
- Park, Y., Lin, K.Y.A., Park, A.H.A., Petit, C., 2015. Recent advances in anhydrous solvents for CO₂ capture: Ionic liquids, switchable solvents, and nanoparticle organic hybrid materials. *Front. Energy Res.* 3. <https://doi.org/10.3389/fenrg.2015.00042>
- Perumal, M., Karunakaran, N.R., Balraj, A., Jayaraman, D., Krishnan, J., Prakash, A.B.J., Arumugam, J., Muthukumar, V.P., 2020. Experimental investigation on CO₂ absorption and physicochemical characteristics of different carbon-loaded aqueous solvents. *Environ. Sci. Pollut. Res.* 28, 63532–63543. <https://doi.org/10.1007/S11356-020-10562-0>
- Poling, B.E., Prausnitz, J.M., O'Connell, J.P., 2001. *Properties of Gases and Liquids*, fifth ed. McGraw-Hill Education, New York. Available: <https://www.accessengineeringlibrary.com/content/book/9780070116825>
- Rafat, A., Atilhan, M., Kahraman, R., 2016. Corrosion behavior of carbon steel in CO₂ saturated amine and imidazolium-, ammonium-, and phosphonium-based ionic liquid solutions. *Ind. Eng. Chem Res.* 55, 446–454. <https://doi.org/10.1021/acs.iecr.5b01794>
- Ramdin, M., de Loos, T.W., Vlugt, T.J.H., 2012. State-of-the-art of CO₂ capture with ionic liquids. *Ind. Eng. Chem. Res.* 51, 8149–8177. <https://doi.org/10.1021/ie3003705>

- Sanku, M.G., Svensson, H., 2019. Modelling the precipitating non-aqueous CO₂ capture system AMP-NMP, using the unsymmetric electrolyte NRTL. *Int. J. Greenh. Gas Control* 89, 20–32. <https://doi.org/10.1016/j.ijggc.2019.07.006>
- Seo, S., Desilva, M.A., Xia, H., Brennecke, J.F., 2015. Effect of cation on physical properties and CO₂ solubility for phosphonium-based ionic liquids with 2-cyanopyrrolide anions. *J. Phys. Chem. B* 119, 11807–11814. <https://doi.org/10.1021/acs.jpcc.5b05733>
- Seo, S., Quiroz-Guzman, M., Desilva, M.A., Lee, T.B., Huang, Y., Goodrich, B.F., Schneider, W.F., Brennecke, J.F., 2014. Chemically tunable ionic liquids with aprotic heterocyclic anion (AHA) for CO₂ capture. *J. Phys. Chem. B* 118, 5740–5751. <https://doi.org/10.1021/jp502279w>
- Song, T., Avelar Bonilla, G.M., Morales-Collazo, O., Lubben, M.J., Brennecke, J.F., 2019. Recyclability of encapsulated ionic liquids for post-combustion CO₂ capture. *Ind. Eng. Chem. Res.* 58, 4997–5007. <https://doi.org/10.1021/acs.iecr.9b00251>
- Torralba-Calleja, E., Skinner, J., Gutiérrez-Tauste, D., 2013. CO₂ capture in ionic liquids: A review of solubilities and experimental methods. *J. Chem.* 2013, 1–16. <https://doi.org/10.1155/2013/473584>
- US–EPA, 2022. State CO₂ Emissions from Fossil Fuel Combustion. <https://www.epa.gov/statelocalenergy/state-co2-emissions-fossil-fuel-combustion> (accessed 15 March 2022).
- Yang, J., Yu, X., Yan, J., Tu, S.T., 2014. CO₂ capture using amine solution mixed with ionic liquid. *Ind. Eng. Chem. Res.* 53, 2790–2799. <https://doi.org/10.1021/ie4040658>

- Zacchello, B., Oko, E., Wang, M., Fethi, A., 2017. Process simulation and analysis of carbon capture with an aqueous mixture of ionic liquid and monoethanolamine solvent. *Int. J. Coal Sci. Technol.* 4, 25–32. <https://doi.org/10.1007/S40789-016-0150-1>
- Zhang, J., Fennell, P.S., Trusler, J.P.M., 2015. Density and viscosity of partially carbonated aqueous tertiary alkanolamine solutions at temperatures between (298.15 and 353.15) K. *J. Chem. Eng. Data* 60, 2392–2399. <https://doi.org/10.1021/acs.jced.5b00282>
- Zhou, S., Wang, S., Chen, C., 2012. Thermal degradation of monoethanolamine in CO₂ capture with acidic impurities in flue gas. *Ind. Eng. Chem. Res.* 51, 2539–2547. <https://doi.org/10.1021/ie202214y>
- Øi, L.E., 2012. Comparison of Aspen HYSYS and Aspen Plus simulation of CO₂ Absorption into MEA from Atmospheric Gas. *Energy Procedia* 23, 360–369. <https://doi.org/10.1016/j.egypro.2012.06.036>